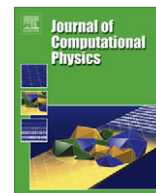




Contents lists available at ScienceDirect

Journal of Computational Physics

journal homepage: www.elsevier.com/locate/jcp

An efficient and robust numerical algorithm for estimating parameters in Turing systems

Marcus R. Garvie^{a,*}, Philip K. Maini^{b,c}, Catalin Trenchea^d^a Department of Mathematics and Statistics, MacNaughton Building, University of Guelph, Guelph, ON, Canada N1G 2W1^b Centre for Mathematical Biology, Mathematical Institute, 24-29 St. Giles', University of Oxford, Oxford OX1 3LB, UK^c Oxford Centre for Integrative Systems Biology, Department of Biochemistry, South Parks Road, Oxford OX1 3QU, UK^d Department of Mathematics, 301 Thackeray Hall, University of Pittsburgh, Pittsburgh, PA 15260, USA

ARTICLE INFO

Article history:

Received 1 March 2010

Received in revised form 21 May 2010

Accepted 28 May 2010

Available online xxx

Keywords:

Optimal control theory

Parameter identification

Reaction–diffusion equations

Diffusion-driven instability

Finite element method

ABSTRACT

We present a new algorithm for estimating parameters in reaction–diffusion systems that display pattern formation via the mechanism of diffusion-driven instability. A Modified Discrete Optimal Control Algorithm (MDOCA) is illustrated with the Schnakenberg and Gierer–Meinhardt reaction–diffusion systems using PDE constrained optimization techniques. The MDOCA algorithm is a modification of a standard variable step gradient algorithm that yields a huge saving in computational cost. The results of numerical experiments demonstrate that the algorithm accurately estimated key parameters associated with stationary target functions generated from the models themselves. Furthermore, the robustness of the algorithm was verified by performing experiments with target functions perturbed with various levels of additive noise. The MDOCA algorithm could have important applications in the mathematical modeling of realistic Turing systems when experimental data are available.

© 2010 Published by Elsevier Inc.

1. Introduction

The Turing reaction–diffusion model (Turing [51]) is the paradigm model for biological pattern formation (see, for example, Murray [39]). This model, a coupled system of parabolic equations, has the counter-intuitive feature that diffusion can drive a spatially uniform stable state unstable leading to spatially non-uniform steady states. Turing termed the reactants “morphogens” and, under the assumption that cells respond to signaling chemicals in a concentration-dependent manner, this model serves to set up a morphogen pre-pattern to determine cell differentiation. This model has been applied to a whole range of patterning phenomena in biology, for example, fish pigmentation patterns [30], shell patterns [36], cartilage formation [37]. The idea of morphogens interacting in this way to form patterns is still controversial, but recent experimental evidence suggests that the Turing model cannot be simply dismissed [48].

Turing patterns have been shown to exist in chemistry [7,40], and in fact the model has been applied in many areas of science. For example, it has been applied in ecology [47] and used as a caricature model by Barrio et al. [3].

The aim of this paper is to present a numerical method for estimating parameters in Turing systems using optimal control theory [42]. Optimal control theory is a mathematical technique used to determine control variables that maximize a per-

* Corresponding author.

E-mail addresses: mgarvie@uoguelph.ca (M.R. Garvie), maini@maths.ox.ac.uk (P.K. Maini), trenchea@pitt.edu (C. Trenchea).

URLs: <http://www.uoguelph.ca/~mgarvie/> (M.R. Garvie), <http://people.maths.ox.ac.uk/~maini/> (P.K. Maini), <http://www.math.pitt.edu/~trenchea/> (C. Trenchea).

formance criterion subject to constraints (state equations). It continues to be an active area of research with applications in many areas [2,15,21,27,31,33,34]. Parameter estimation and data assimilation problems can be formulated in this context by seeking model parameters corresponding to state variables that “best approximate” observed data in some sense, for example least squares. When a cost functional measuring the discrepancy between solutions and target functions is formulated, constrained optimization techniques are employed (one-shot, sensitivity or adjoint-based methods) to construct an iterative algorithm [10,29] for estimating model parameters. There are numerous works in the literature that apply optimal control theory to reaction–diffusion systems [4–6,8,12,13,16,19,20,45]. However, relatively few works focus on estimating parameters in nonlinear reaction–diffusion systems [1,14,24,28], and to the best of our knowledge, none address parameter estimation for the Turing reaction–diffusion model. It is in this area of knowledge that our paper contributes. The main challenge in parameter estimation for Turing models is that the solution of such systems typically requires numerical integration over a large time interval $[0, T]$ with many small time-steps Δt . The methodology presented in this paper capitalizes on the fact that the target functions are stationary, which results in an algorithm with a vast reduction in computational cost compared to the standard optimal control approach.

The structure of our paper is outlined as follows. In Section 2 the governing reaction–diffusion systems (‘state equations’) are introduced and a Direct Problem defined where we seek morphogen concentrations associated with given key parameters. In Section 3 the Inverse Problem is defined where we seek to recover the key model parameters that led to given target morphogen concentrations. The mathematical theory of optimal control is then used to derive an optimality system, which allows us to characterize the optimal (‘key’) parameters of the systems in terms of adjoint variables (see Section 4). In Section 5 we discuss the numerical methods used to approximate the state and adjoint equations, construction of the target functions, and implementation of a Modified Discrete Optimal Control Algorithm (MDOCA). The results of some numerical experiments are presented in Section 6 and the results and implications discussed in Section 7.

2. Direct problem

We study coupled pairs of reaction–diffusion equations, called the ‘state equations’, with the following general non-dimensional form:

$$\begin{cases} \frac{\partial u}{\partial t} = D_u \nabla^2 u + f_1(u, v), \\ \frac{\partial v}{\partial t} = D_v \nabla^2 v + f_2(u, v), \end{cases} \quad (1)$$

where $u(\mathbf{x}, t)$ and $v(\mathbf{x}, t)$ are morphogen concentrations at (vector) position $\mathbf{x} = (x, y)^T \in \Omega$ and time $t \in (0, T)$. Here Ω is a bounded domain in \mathbb{R}^2 . D_u and D_v are the positive diffusion coefficients of u and v , respectively. The standard Laplacian operator in two space dimensions is given by $\nabla^2 = \partial^2/\partial x^2 + \partial^2/\partial y^2$. The functions f_1 and f_2 model the reaction kinetics of u and v . We assume there is no flux of the morphogen concentrations across the boundary of Ω and that the initial concentrations, $u_0(\mathbf{x})$, $v_0(\mathbf{x})$, are bounded and positive. To illustrate our methodology we focus on the following nonlinear examples of f_1 and f_2 :

(i) the Schnakenberg [46] model (first proposed by Gierer and Meinhardt [18]):

$$f_1(u, v) := \gamma(a - u + u^2 v), \quad f_2(u, v) := \gamma(b - u^2 v), \quad (2)$$

where γ , a and b are positive constants.

(ii) the Gierer and Meinhardt [18] model:

$$f_1(u, v) := \frac{ru^2}{v} - \mu u + r, \quad f_2(u, v) := ru^2 - \alpha v, \quad (3)$$

where r , μ and α are positive constants.

The aim of this paper is to estimate key parameters associated with patterns arising via diffusion-induced instability. For concreteness we focus on parameters c_1 and c_2 where:

$$\begin{aligned} c_1 = a, \quad c_2 = b & \text{ in the Schnakenberg model,} \\ c_1 = \mu, \quad c_2 = \alpha & \text{ in the Gierer–Meinhardt model.} \end{aligned}$$

It is natural to assume pointwise bounds on the parameters, and thus we restrict the parameters to the admissible set:

$$\mathcal{U}_{ad} = \{(c_1, c_2) \in \mathbb{R}^2 : 0 < c_1 \leq C_1, 0 < c_2 \leq C_2\}, \quad (4)$$

where C_1 and C_2 are determined from knowledge of the Turing spaces of the systems concerned. We now state the direct problem:

(DP) For given parameters (c_1, c_2) belonging to the admissible set \mathcal{U}_{ad} , find the morphogen concentrations $u(\mathbf{x}, t)$ and $v(\mathbf{x}, t)$ satisfying (1) with kinetics (i) or (ii) for all $(\mathbf{x}, t) \in \Omega \times [0, T]$.

In order to prove a technique for the identification of parameters in our method (see Garvie and Trenchea [17]), it is necessary that the solutions of the reaction–diffusion system (1) exist, are unique, are positive and depend continuously on the initial data. In the case of kinetics (i) as we were unable to find a proof in the literature we provide a proof in Appendix A.1. In the case of kinetics (ii), existence and uniqueness are proved in the monograph by Rothe [43], and the positivity of solutions follows from an analogous argument to the one given for kinetics (i).

3. Inverse problem statement and parameter identification

The basic description of the inverse problem is as follows. We start with given stationary ‘target functions’ (\bar{u}, \bar{v}) that represent some desired morphogen concentrations of the system (a ‘pattern’). We then seek the key parameters such that the solution of the Direct Problem (DP) (u, v) matches the target functions (\bar{u}, \bar{v}) as closely as possible.

The target functions may be noisy due to measurement error, or may not be a solution of the Direct Problem (DP). Thus we employ a least-squares technique so that (u, v) best approximates (\bar{u}, \bar{v}) . The basic optimal control technique is to minimize a quadratic cost functional subject to the reaction–diffusion system as a constraint.

Denoting the Banach space of square integrable functions over $\Omega_T := \Omega \times (0, T)$ by $L^2(\Omega_T)$, for given \bar{u} and \bar{v} in $L^2(\Omega_T)$, the least-squares approach leads to the minimization problem:

$$\inf_{c_1, c_2 \in \mathcal{U}_{ad}} J(c_1, c_2), \quad (5)$$

where the cost functional J is defined by:

$$J(c_1, c_2) = \frac{1}{2} \int_{\Omega} (\gamma_1 |u(x, T) - \bar{u}(x)|^2 + \gamma_2 |v(x, T) - \bar{v}(x)|^2) dx + \frac{\delta_1}{2} c_1^2 + \frac{\delta_2}{2} c_2^2, \quad (6)$$

subject to the reaction–diffusion system (1) as a constraint. The terms weighted by γ_i measure the discrepancy between the solution and targets at the final time T . The terms weighted by δ_i effectively bound the size of the key parameters c_1 and c_2 , which is a requirement of (4) and also allow for possibly noisy data. The use of the terms weighted by δ_i is called Tikhonov regularization (Engl et al. [11]) and circumvents the possibly ill-posedness of the inverse problem associated with the partial differential equations (Isakov [26], Tikhonov and Arsenin [50]). There are various ways to choose the regularization parameters, for example, via the L -curve method, however a discussion of the optimal choice of these parameters is outside the scope of this paper (see [52] for further details).

By appropriately choosing the weights in the cost functional we can place more emphasis on the solutions matching the targets, or we can place more emphasis on limiting the size of the parameters.

We now state the inverse problem for parameter identification in the reaction–diffusion system (1) with kinetics (i) or (ii):

(IP) For given target functions $\bar{u}, \bar{v} \in L^2(\Omega)$, find optimal parameters $(c_1^*, c_2^*) \in \mathcal{U}_{ad}$ and optimal solutions (u^*, v^*) of (1) that satisfy the minimization problem (5).

The rigorous proof of the existence of a solution to the inverse problem (IP) for the reaction–diffusion system (1) with kinetics (3) is given by Garvie and Trenchea [17] and first-order necessary conditions for optimality are used to derive an optimality system of partial differential equations whose solutions provide optimal states and controls. The corresponding results for the simpler system with the Schnakenberg kinetics (2) are proved in a similar fashion.

4. Optimality system

The mathematical theory of optimal control theory leads to the derivation of a linear reaction–diffusion system for ‘adjoint’ variables $(p(\mathbf{x}, t), q(\mathbf{x}, t))$ called the ‘adjoint system’:

$$\begin{cases} -\frac{\partial p}{\partial t} = D_u \nabla^2 p + g_1(p, q), \\ -\frac{\partial q}{\partial t} = D_v \nabla^2 q + g_2(p, q), \end{cases} \quad (7)$$

corresponding to the system for the Lagrange multipliers of the PDE constrained optimization problem. Corresponding to kinetics (i) we have:

$$g_1(p, q) := 2\gamma u v (p - q) - \gamma p, \quad g_2(p, q) := \gamma u^2 (p - q), \quad (8)$$

and corresponding to kinetics (ii) we have:

$$g_1(p, q) := \left(2r \frac{u}{v} - \mu\right)p + 2ruq, \quad g_2(p, q) := -r \frac{u^2}{v^2}p - \alpha q. \quad (9)$$

The adjoint equations are backward in time and thus terminal conditions are needed instead of initial conditions:

$$p(\cdot, T) = \gamma_1(u(\cdot, T) - \bar{u}(\cdot)), \quad q(\cdot, T) = \gamma_2(v(\cdot, T) - \bar{v}(\cdot)). \quad (10)$$

We also use the adjoint system to obtain an explicit characterization of the optimal controls in terms of the adjoint variables, which are called ‘optimality conditions’:

$$\begin{aligned} c_1^* &= \max \left\{ 0, \min \left\{ \frac{1}{\delta_1} \int_{\Omega_T} d_1 p \, dxdt, C_1 \right\} \right\}, \\ c_2^* &= \max \left\{ 0, \min \left\{ \frac{1}{\delta_2} \int_{\Omega_T} d_2 q \, dxdt, C_2 \right\} \right\}, \end{aligned} \quad (11)$$

where with kinetics (i) $d_1 = d_2 = -\gamma$, and with kinetics (ii) $d_1 := u^*$, $d_2 := v^*$. The state equation (1), and the adjoint equation (7) together with the optimality conditions are called the ‘optimality system’ (see Appendix A.2). For mathematical details concerning derivation of the optimality systems see the works by Lenhart and Workman [33], Garvie and Trenchea [17].

5. Numerical methods

5.1. Approximation of the state and adjoint equations

We approximate the state equations and adjoint equations on the unit square using an unstructured grid generator. In all our simulations we partition the domain into 8192 approximately equilateral triangles with 4225 nodes and then apply the standard Galerkin finite element method (Ciarlet [9]) with piecewise linear continuous basis functions. For a given generic reaction–diffusion equation of the form:

$$\frac{\partial u}{\partial t} = D \nabla^2 u + f(u),$$

where D is the diffusion coefficient for a morphogen u , application of the finite element method leads to a large system of ordinary differential equations (an Initial Value Problem (IVP)) in the form:

$$\dot{\mathbf{U}} = D \nabla_h^2 \mathbf{U} + \mathbf{F}(\mathbf{U}),$$

where ∇_h^2 is the discrete Laplacian depending on a (spatial) step-size h .

For the time discretization of the IVP it is well-known that several popular time-stepping schemes for reaction–diffusion equations modeling pattern formation yield qualitatively poor results (Ruuth [44]). In order to approximate the reaction–diffusion system with kinetics (i) we employed the following ‘first-order semi-implicit backward Euler difference scheme’ (1-SBEM):

$$\begin{cases} \frac{u^{n+1} - u^n}{\Delta t} = D_u \nabla^2 u^{n+1} + \gamma(a - u^{n+1} + u^n u^{n+1} v^n), \\ \frac{v^{n+1} - v^n}{\Delta t} = D_v \nabla^2 v^{n+1} + \gamma(b - (u^n)^2 v^{n+1}), \end{cases} \quad (12)$$

where Δt is the uniform time-step of the time interval $[0, T]$ and n refers to the n th time level at time $t_n := n\Delta t$. Note that the diffusion and linear components of the reaction kinetics are approximated implicitly, while the nonlinear components are treated semi-implicitly. This scheme was successfully used by Madzvamuse [35] to accurately simulate Turing patterns of the Schnakenberg system.

To solve the reaction–diffusion system with kinetics (ii) we employed a second order, 3-level, implicit–explicit (IMEX) scheme (2-SBDF) recommended by Ruuth [44] as a good choice for most reaction–diffusion problems for pattern formation, namely:

$$\begin{cases} \frac{3u^{n+1} - 4u^n + u^{n-1}}{2\Delta t} - D_u \nabla^2 u^{n+1} = 2f_1(u^n, v^n) - f_1(u^{n-1}, v^{n-1}), \\ \frac{3v^{n+1} - 4v^n + v^{n-1}}{2\Delta t} - D_v \nabla^2 v^{n+1} = 2f_2(u^n, v^n) - f_2(u^{n-1}, v^{n-1}), \end{cases} \quad (13)$$

where f_1 and f_2 are given by the Gierer–Meinhardt kinetics (3). One of the advantages of this scheme is that we can use relatively large time-steps and still obtain a good approximation of highly oscillatory solutions. IMEX schemes use an implicit discretization of the diffusion term, and an explicit discretization of the reaction terms. As the scheme 2-SBDF involves three time levels we approximate the solutions at the first time level using a first-order IMEX scheme (1-SBDF) with a small time-step (Ruuth [44]).

The numerical schemes used to approximate the linear adjoint equations were similar to the schemes used to approximate the state equations. Application of the finite element method for the spatial discretization coupled with the time-stepping

schemes in all cases led to sparse linear systems of algebraic equations, which were solved in MATLAB (R2008a) using the GMRES iterative solver.

5.2. Construction of the target functions

The target functions (\bar{u}, \bar{v}) used in this paper were generated from the reaction–diffusion systems themselves via the mechanism of diffusion-driven instability (the ‘Turing mechanism’). Solutions were generated on the unit square with homogeneous Neumann boundary conditions. The standard approach in the literature for constructing Turing patterns is to prescribe the initial data equal to small random perturbations about the corresponding stationary states of the spatially homogeneous systems, i.e. the reaction–diffusion systems without diffusion. The problem with this approach is that this is often done using an unspecified random number generator with an unspecified ‘seed’, and thus the numerical results are effectively not reproducible. To circumvent this problem we perturb the stationary states using known functions. For kinetics (i) we choose the initial conditions (see Ruuth [44], or Madzvamuse [35]):

$$u(\mathbf{x}, 0) = 0.919145 + 0.0016 \cos(2\pi(x + y)) + 0.01 \sum_{j=1}^8 \cos(2\pi jx),$$

$$v(\mathbf{x}, 0) = 0.937903 + 0.0016 \cos(2\pi(x + y)) + 0.01 \sum_{j=1}^8 \cos(2\pi jx),$$

while the initial conditions for kinetics (ii) were chosen equal to the same functions, but with the ‘cosine’ function replaced with the ‘sine’ function.

The state equations were solved until the transient solutions died out, which was determined by waiting until some large time $t = T$ when the l_2 norm of the change in state in one time-step was less than some small tolerance. We checked that the patterns were unchanged at $t = 2T$, thus confirming that the solutions were indeed stationary. Target functions for u are shown in Fig. 1 (the patterns for v are similar). See the caption for the parameter values.

5.3. Discrete optimal control procedure

5.3.1. The standard algorithm

To approximate the Inverse Problem (IP) we applied a ‘variable step gradient algorithm’ yielding a sequence of approximations to the optimal solutions and optimal parameters (Ciarlet [10], Garvie and Trenchea [17], Gunzburger [21], Gunzburger and Manservigi [22]). The pseudo-code for the standard algorithm is given in Algorithm 1. Algorithm 1 is applied to the discrete State Equations (SE), discrete Adjoint Equations (AE) and discrete objective functional at the final time-step t_N . We begin by making an initial guess for the parameters $c_1(0)$, $c_2(0)$ and starting values for the step length λ and a prescribed tolerance ε used to test the convergence of the cost functional. Initial conditions for the states, namely (u_0, v_0) , were chosen to be the same as the initial conditions used to generate the target functions (see Section 5.2). Then for each iteration k of the gradient method we solve the nonlinear reaction–diffusion system for $u(k)$, $v(k)$ ($k \geq 1$), and store the cost $J(c_1(k), c_2(k))$. We also compute the adjoint variables $p(k)$, $q(k)$, determine $dJ(c_1(k), c_2(k))/d(c_1(k), c_2(k))$, the total derivative of J with respect to

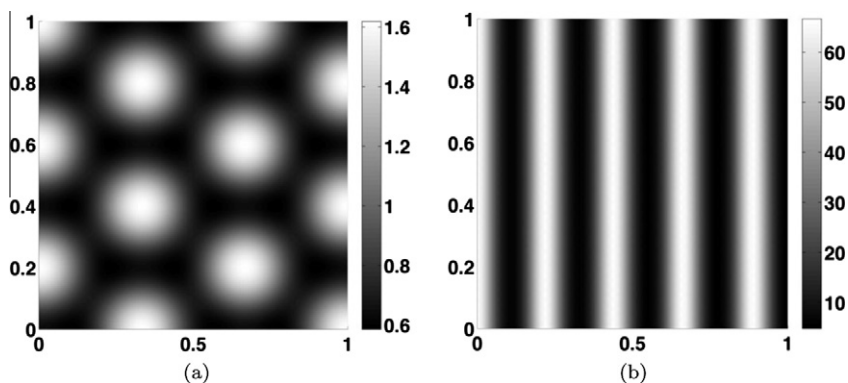


Fig. 1. (a) Target function \bar{u} for the Schnakenberg kinetics: $T = 5$, $D_u = 1$, $D_v = 10$, $\gamma = 1000$, $a = 0.126779$, $b = 0.792366$, $\Delta t = 0.0001$ (1-SBEM). (b) Target function \bar{u} for the Gierer–Meinhardt kinetics: $T = 238.853$, $D_v = 0.27$, $D_u = 9.45 \times 10^{-4}$, $r = 0.001$, $\alpha = 100$, $\mu = 2.5$, $\Delta t = 1 \times 10^{-8}$ (1-SBDF), $\Delta t = 0.001$ (2-SBDF). For details concerning the finite element methods and initial and boundary conditions see the main text above.

the vector $(c_1(k), c_2(k))$, and take a step along this direction using the appropriate step length λ , provided the cost functional decreases. If the cost functional fails to decrease, then the step length is rejected and the step length decreased. If the step length is accepted, then the parameters $(c_1(k), c_2(k))$ are updated using a Standard Gradient Update (SGU):

$$(c_1(k), c_2(k)) = (c_1(k-1), c_2(k-1)) - \lambda \frac{dJ(c_1(k-1), c_2(k-1))}{d(c_1(k-1), c_2(k-1))}, \quad k \geq 1. \quad (14)$$

The procedure is repeated until the relative change in the cost is smaller than the tolerance ε , namely:

$$\left| \frac{J^N(k) - J^N(k-1)}{J^N(k)} \right| \leq \varepsilon, \quad (15)$$

where $J^N(k)$ refers to the cost at time level N at iteration k . In order to take into account possible stagnation of the iterative method¹ we exit the algorithm if the step length λ becomes smaller than the tolerance ε . The iterative method is computationally expensive as each iteration of the discrete optimal control algorithm requires the numerical solution of the state equation up to some final time $T = N\Delta t$, the numerical solution of the adjoint equations backward in time from T , and gradient updates.

Algorithm 1. Standard gradient algorithm

initialization

$k \leftarrow 0$;
 $RelError \leftarrow 1000$ {Arbitrary large starting value};
 Choose initial guess $(c_1(0), c_2(0))$, λ , and ε ;
for $n = 1, \dots, N$ **do**
 solve SE for $(u^n(0), v^n(0))$, with $(u^0(0), v^0(0)) = (u_0, v_0)$;

end for

evaluate $J^N(0)$;

$\lambda \leftarrow 2\lambda/3$;

end initialization

main loop

while $RelError > \varepsilon$ **do**

$\lambda \leftarrow 3\lambda/2$;

$k \leftarrow k + 1$;

for $n = N - 1, \dots, 0$ **do**

 solve AE for $(p^n(k), q^n(k))$, with $(p^N(k), q^N(k))$;

end for

 solve SGU for $(c_1(k), c_2(k))$;

for $n = 1, \dots, N$ **do**

 solve SE for $(u^n(k), v^n(k))$, with $(u^0(k), v^0(k)) = (u_0, v_0)$;

end for

 evaluate $J^N(k)$;

while $J^N(k) \geq J^N(k-1)$ **do**

$\lambda \leftarrow \lambda/2$;

if $\lambda < \varepsilon$ **do**

 print ('Algorithm stagnated')

end if

 solve SGU for $(c_1(k), c_2(k))$;

for $n = 1, \dots, N$

 solve SE for $(u^n(k), v^n(k))$, with $(u^0(k), v^0(k)) = (u_0, v_0)$;

end for

 evaluate $J^N(k)$;

end while

$RelError \leftarrow |J^N(k) - J^N(k-1)|/|J^N(k)|$

end while

end main loop

¹ For example, when the cost functional is approximately flat.

5.3.2. A modified discrete optimal control algorithm

We present a Modified Discrete Optimal Control Algorithm (MDOCA) based on a modification of the standard algorithm discussed above. The pseudo-code for the MDOCA is given in Algorithm 2. The MDOCA algorithm takes advantage of the fact that the target functions are stationary solutions of the state equations. As the target functions are known data, we choose the initial data of the state equations equal to the target functions, take the final time T equal to only two time steps² Δt , and seek parameters $c_1(k)$ and $c_2(k)$ that correspond to stationary initial data. The other steps of the MDOCA algorithm are essentially the same as in the standard algorithm. If the parameters $c_1(k)$ and $c_2(k)$ are optimal, then the cost after two time-steps $2\Delta t$ is zero and the algorithm stops. If the parameters $c_1(k)$ and $c_2(k)$ are suboptimal, then the initial data evolve over two time-steps $2\Delta t$. The discrepancy between the solutions and targets is then measured by the cost functional and the modified variable step gradient algorithm adjusts the parameters accordingly.

Algorithm 2. Modified gradient algorithm (MDOCA)

```

initialization    $k \leftarrow 0$ ;
                   $RelError \leftarrow 1000$  {Arbitrary large starting value};
                  Choose initial guess  $(c_1(0), c_2(0))$ ,  $\lambda$ , and  $\varepsilon$ ;
                  for  $n = 1, 2$  do
                      solve SE for  $(u^n(0), v^n(0))$ , with  $(u^0(0), v^0(0)) = (\bar{u}, \bar{v})$ ;
                  end for
                  evaluate  $J^2(0)$ ;
                   $\lambda \leftarrow 2\lambda/3$ ;
end initialization
main loop
while  $RelError > \varepsilon$  do
     $\lambda \leftarrow 3\lambda/2$ ;
     $k \leftarrow k + 1$ ;
    for  $n = 1, 0$  do
        solve AE for  $(p^n(k), q^n(k))$ , with  $(p^2(k), q^2(k))$ ;
    end for
    solve SGU for  $(c_1(k), c_2(k))$ ;
    for  $n = 1, 2$  do
        solve SE for  $(u^n(k), v^n(k))$ , with  $(u^0(k), v^0(k)) = (\bar{u}, \bar{v})$ ;
    end for
    evaluate  $J^2(k)$ ;
    while  $J^2(k) \geq J^2(k-1)$  do
         $\lambda \leftarrow \lambda/10$ ;
        if  $\lambda < \varepsilon$  do
            print ('Algorithm stagnated')
        end if
        solve SGU for  $(c_1(k), c_2(k))$ ;
        for  $n = 1, \dots, N$  do
            solve SE for  $(u^n(k), v^n(k))$ , with  $(u^0(k), v^0(k)) = (\bar{u}, \bar{v})$ ;
        end for
        evaluate  $J^2(k)$ ;
    end while
     $RelError \leftarrow |J^2(k) - J^2(k-1)|/|J^2(k)|$ 
end while
end main loop

```

6. Numerical results

6.1. Experiments with the MDOCA algorithm

We were unable to obtain satisfactory results using the standard algorithm as the iterative procedure failed to converge and frequently stagnated, yielding parameter values far from the optimal ones (results not presented). However, the MDOCA algorithm converged for almost all starting values ('initial guesses') that we chose for the key parameters c_1 and c_2 , taking on the order of half a minute to accurately estimate the optimal parameters used to generate the target patterns (using Matlab 7.6.0 (R2008a) on a Mac Pro with a 2×3 GHz Dual-Core Intel Xeon processor). Table 1 shows the results of one experiment

² Two time-steps are the minimum number of time-steps that the discrete optimal control procedure needs to run.

Table 1

Parameter estimates for the modified algorithm.

Parameter	Start value	Estimated value	Optimal value	% Rel error
a	5	0.126776	0.126779	2.4×10^{-3}
b	0.3	0.792365	0.792366	1.3×10^{-4}
μ	50	2.499375	2.5	2.5×10^{-2}
α	30	100.045529	100	4.6×10^{-2}

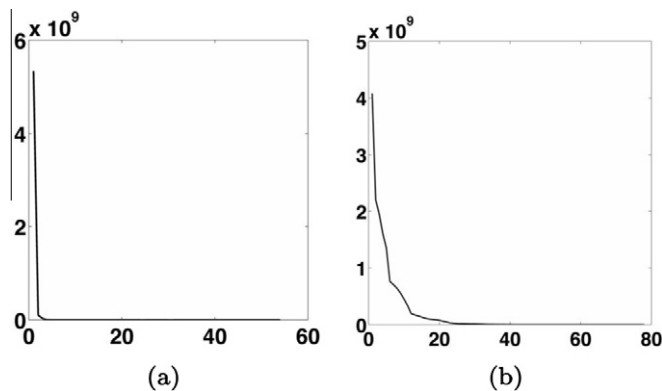


Fig. 2. Change in cost with iteration count. (a) Schnakenberg system: $D_u = 1$, $D_v = 10$, $\gamma = 1000$, $\Delta t = 0.0001$ (1-SBEM), $\gamma_1 = \gamma_2 = 1 \times 10^{10}$, $\delta_1 = \delta_2 = 1$. (b) Gierer–Meinhardt system: $D_v = 0.27$, $D_u = 9.45 \times 10^{-4}$, $r = 0.001$, $\Delta t = 1 \times 10^{-8}$ (1-SBDF), $\Delta t = 0.001$ (2-SBDF), $\gamma_1 = 5.5 \times 10^9$, $\gamma_2 = 1 \times 10^{15}$, $\delta_1 = \delta_2 = 0$.

for each system. We obtained more significant figures of accuracy when estimating a and b than when estimating μ and α , which was generally the case. To verify convergence we also plotted the cost functional against iteration count for both reaction–diffusion systems. The plots show an initial rapid decrease in cost with a subsequent slow decrease after the first few iterations of the optimal control algorithm (see Fig. 2 and the caption for the remaining parameters used in the simulations). We also checked that the solutions at the final time T corresponding to the exact parameters and the estimated parameters (see Table 1) were the same.

6.2. Robustness of the MDOCA algorithm

To test the robustness of the MDOCA algorithm, we repeated the experiments of Section 6.1 with perturbing target functions \bar{u} and \bar{v} . The target functions for the Schnakenberg and Gierer–Meinhardt systems (see Fig. 1) were perturbed at every point on the computational grid by adding pseudo random numbers³ drawn from a Normal distribution with mean 0 and standard deviation σ . As the ranges for \bar{u} and \bar{v} differ significantly, to add a comparable level of noise to both targets, we chose σ equal to $s\%$ of the range of the exact target functions, namely, for the target \bar{u} :

$$\sigma = \frac{s}{100} \left[\max_{(x,y) \in [0,1]^2} \bar{u}(x,y) - \min_{(x,y) \in [0,1]^2} \bar{u}(x,y) \right] \quad \text{with } s = 0, 1, 5, 10, 20, 50,$$

and similarly for \bar{v} . Taking $s = 0$ corresponds to the ‘exact’ target functions with no added noise. Negative values of the perturbed target functions were truncated to machine epsilon (approximately 2.22×10^{-16} in Matlab 7.6.0 (R2008a)).

The perturbed target functions are shown in Fig. 3 (for $s = 5, 10, 50$), and the parameter estimates for various levels of noise are displayed in Tables 2 and 3. The percent relative errors are given (to 2 s.f.) with respect to the optimal parameter values (see Table 1). Similar results were obtained using pseudo random numbers⁴ drawn from an uniform distribution to perturb the target functions up to a maximum of $\pm 50\%$ at every point on the computational grid (results not shown).

To test how well the parameters estimated from noisy data can be used to recover the target functions without noise, we solved both the Schnakenberg and Gierer–Meinhardt reaction–diffusion until the final times T using the estimated parameters given in Tables 2 and 3. Fig. 4 shows the solutions u for various levels of noise.

³ Using the intrinsic function RANDN in Matlab 7.6.0 (R2008a).

⁴ Using the intrinsic function RAND in Matlab 7.6.0 (R2008a).

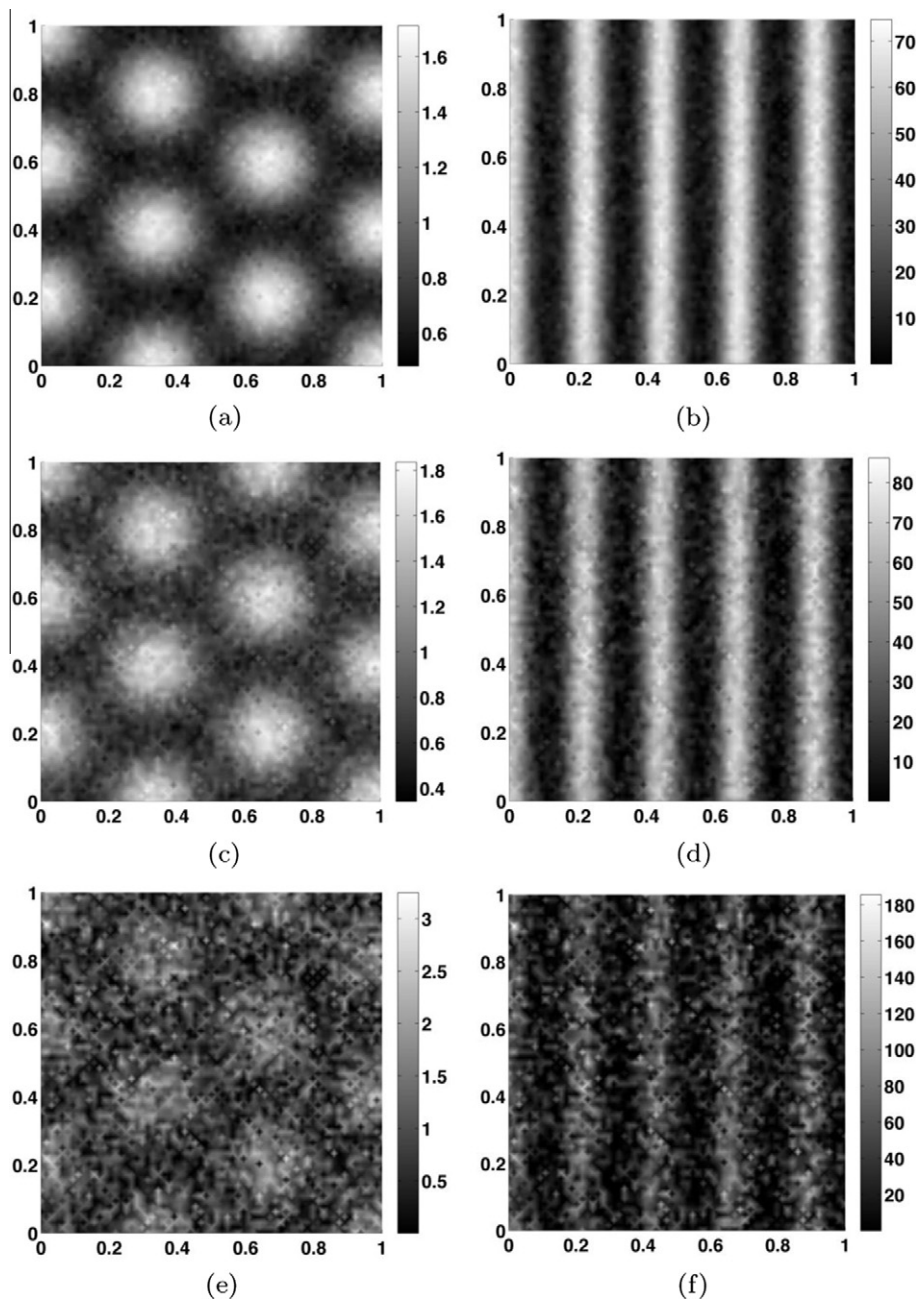


Fig. 3. Targets functions \bar{u} generated from the Schnakenberg system (1st column figures) and the Gierer–Meinhardt system (2nd column figures) with various levels of additive noise using pseudo random numbers drawn from a Normal distribution with mean 0 and standard deviation σ equal to $s\%$ of the range of the exact targets (see Fig. 1): (a) and (b) $s = 5\%$, (c) and (d) $s = 10\%$, (e) and (f) $s = 50\%$. Negative values are truncated to machine epsilon (approximately 2.22×10^{-16} in Matlab 7.6.0 (R2008a)). For all other parameter values see Fig. 1.

Table 2

Parameter estimates for the Schnakenberg system with various levels of s .

s	a	% Rel error	b	% Rel error
0	0.126776	2.4×10^{-3}	0.792365	1.3×10^{-4}
10	0.122131	3.7	0.804886	1.6
20	0.112044	12	0.829722	4.7
30	0.096992	23	0.868733	9.6
40	0.083251	34	0.920127	16
50	0.050569	60	0.989965	25
60	0.020644	84	1.071871	35
70	0	100	1.153198	46

Table 3Parameter estimates for the Gierer–Meinhardt system with various levels of s .

s	α	% Rel error	μ	% Rel error
0	100.045529	0.046	2.499375	0.025
5	101.516086	1.5	2.480466	0.78
10	104.990654	5.0	2.307840	7.7
15	108.445092	8.4	2.377437	4.9
20	113.064953	13	2.327029	6.9
25	36.306046	64	$>5.2 \times 10^{10}$	$>2.1 \times 10^{11}$

The results in Tables 2 and 3 verify that the MDOCA algorithm successfully yields parameter estimates from noisy data. In the Schnakenberg case, the percent relative error in the parameter estimates increases roughly linearly with increasing levels of noise added. In the Gierer–Meinhardt case the pattern is less clear-cut, and with noise levels above a certain critical value

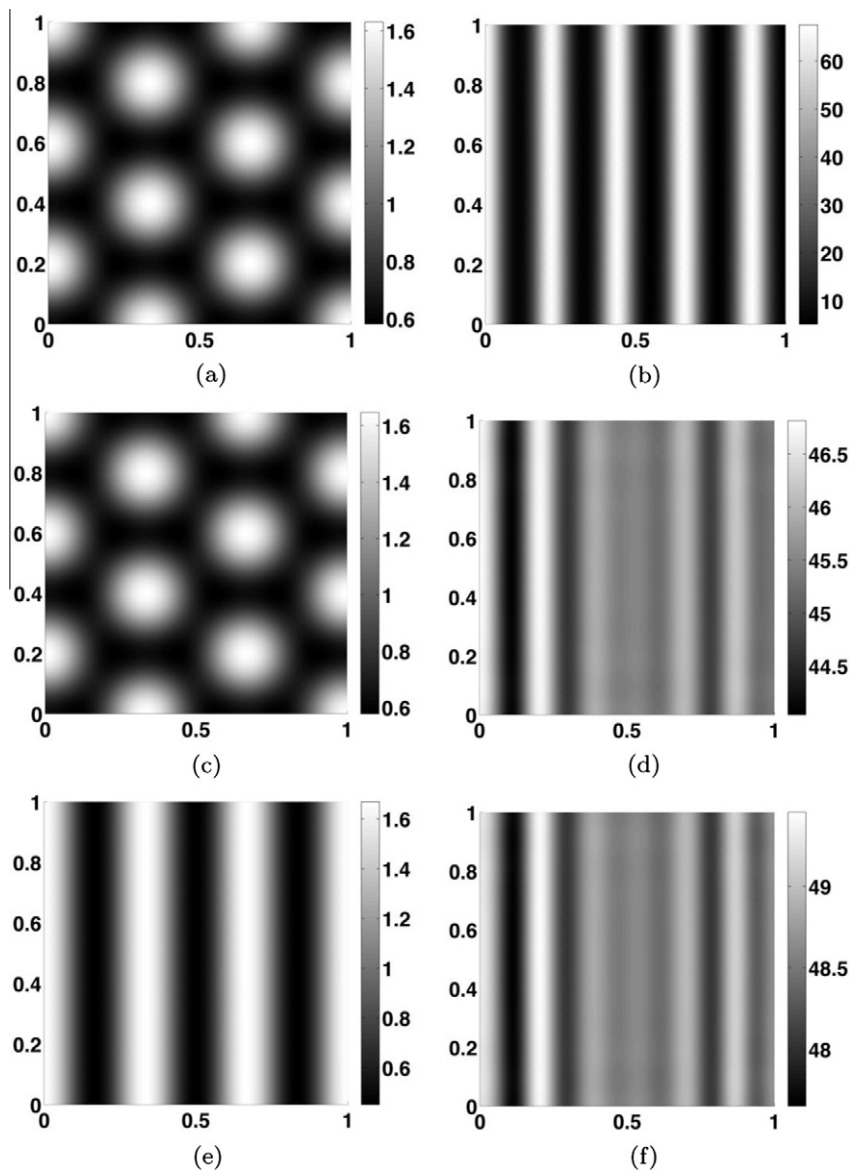


Fig. 4. Solutions u for the Schnakenberg system (1st column figures) and the Gierer–Meinhardt system (2nd column figures) using the estimated parameters from Tables 2 and 3: (a) and (b) $s = 5$, (c) and (d) $s = 10$, (e) $s = 50$, (f) $s = 20$. For the remaining parameters see Fig. 2.

($s \geq 25$) the parameter estimates degrade rapidly. However with modest levels of noise in the data (approximately $s \leq 15$), the modified algorithm applied to both systems yields reasonable parameter estimates (relative errors less than 10%).

The robustness of the MDOCA algorithm was demonstrated by solving the state equations with parameters estimated from noisy data. With noise levels corresponding to about $s = 10$ in the Schnakenberg case and $s = 5$ in the Gierer–Meinhardt case, the target functions without noise were accurately recovered (see Fig. 4).

6.2.1. Sensitivity of pattern formation on model parameters

Once the optimal parameters of a system have been accurately found we can investigate how sensitive the patterns are to changes in the parameters. For fixed target patterns we plotted the surfaces corresponding to the cost as a function of the parameters in the Schnakenberg and Gierer–Meinhardt reaction–diffusion systems (see Fig. 5). We can see from Fig. 5(a) that the target pattern is relatively insensitive to changes in a compared to changes in b . Similarly, we can see from Fig. 5(b) that the target pattern is relatively insensitive to changes in α compared to changes in μ . The insensitivity of a pattern to changes in a model parameter tells us that there exists a family of similar patterns in a neighborhood of the optimal pair (c_1^*, c_2^*) . For example, in Fig. 5(b) if we fix μ at its optimal value $\mu^* = 2.5$, then we expect the patterns associated with the points $(2.5, \alpha)$, $\alpha \in \mathbb{R}$, to be similar, provided we are close to the optimal pair $(2.5, 100)$. This is verified in Fig. 6, which shows the patterns associated with points close to the optimal parameter pair (μ^*, α^*) , where we have

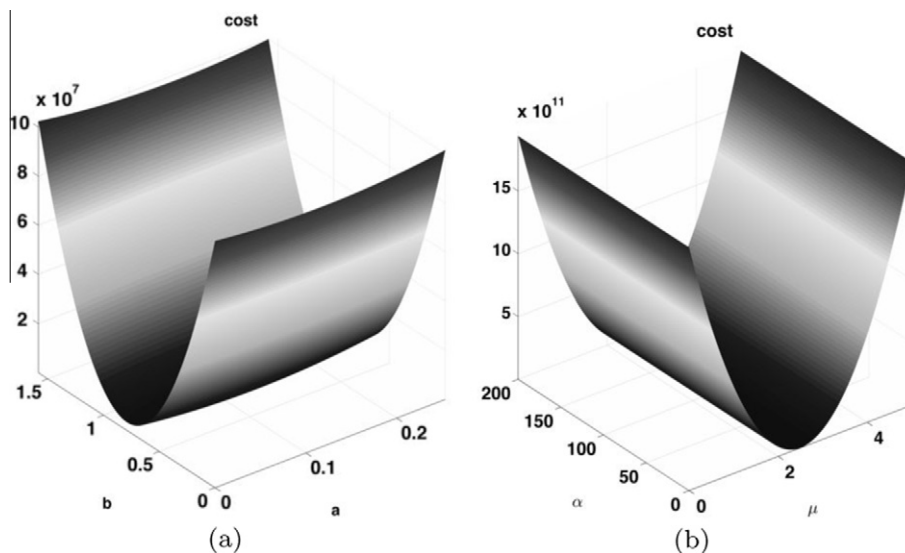


Fig. 5. (a) The cost functional as a function of the parameters c_1 and c_2 for (a) the Schnakenberg system, and (b) the Gierer–Meinhardt system. The surfaces were plotted using 200×200 points in the $c_1 - c_2$ plane.

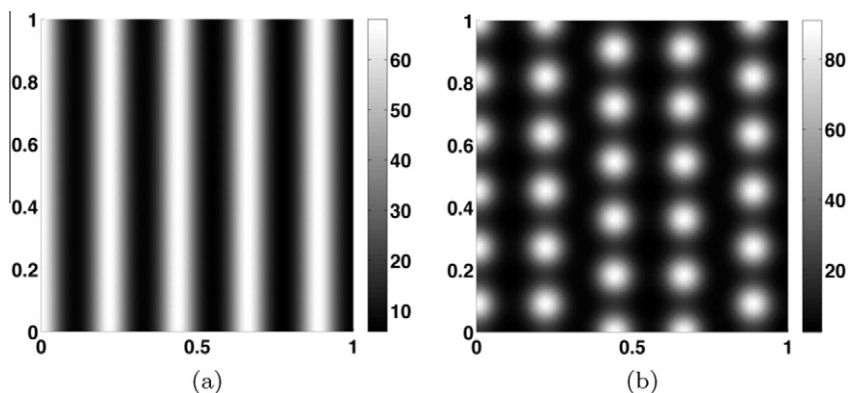


Fig. 6. Morphogen concentrations u for the Gierer–Meinhardt system with $T = 238.853$, $D_v = 0.27$, $D_u = 9.45 \times 10^{-4}$, $r = 0.001$, $\Delta t = 1 \times 10^{-8}$ (1-SBDF), $\Delta t = 0.001$ (2-SBDF). (a) $\alpha = 90$, $\mu = 2.5$, (b) $\alpha = 100$, $\mu = 2.4$. For details concerning the finite element methods and initial and boundary conditions see the main text above.

perturbed either μ^* or α^* . As predicted, the pattern in Fig. 6(a) is very similar to the target pattern in Fig. 1(b), unlike the pattern in Fig. 6(b) that is very different.

7. Conclusion

In this paper we presented a Modified Discrete Optimal Control Algorithm (MDOCA) for the accurate and efficient estimation of parameters used to generate patterns via the mechanism of diffusion-driven instability. Unlike previous studies, which rely on linear analysis of parameter estimation in Turing systems, with the assumption that these will predict the form of patterns in the nonlinear regime, the modified algorithm is based on the rigorous mathematical theory of optimal control theory and provides a systematic and reliable approach to parameter estimation. The methodology is illustrated with the Schnakenberg and Gierer–Meinhardt reaction–diffusion systems where two key parameters are estimated in each model. The robustness of the algorithm was also verified. We demonstrating the ability of the algorithm to yield reasonable estimates of the model parameters, with perturbed target functions using various levels of additive noise.

The MDOCA algorithm not only improves significantly the standard variable step gradient algorithm, but might also prove useful when coupled with linear stability analysis in order to determine parameter values necessary for the formation of spatial structure. Furthermore, it offers the possibility of deriving parameters for patterns exhibited far from primary bifurcation points where linear stability analysis is no longer valid.

The novelty of our numerical procedure is due to the manner in which we modified a standard variable step gradient algorithm for updating the control variables in a discrete optimal control procedure. We take advantage of the fact that the target functions are stationary solutions by choosing the initial data equal to the target functions. As a consequence of this choice, each iteration of the MDOCA algorithm requires only two time-steps for the solution of the state and adjoint equations, which is a huge saving in computational cost compared to the standard optimal control procedure. The standard optimal control procedure typically requires time integration with small time-steps over a large time interval $[0, T]$.

There are some limitations of the MDOCA algorithm. Firstly, it cannot be used to estimate parameters associated with non-stationary target functions. Furthermore, if the target functions are not sufficiently ‘close’ to a solution of the reaction–diffusion systems, the algorithm may fail to converge, or yield highly inaccurate estimates of the model parameters. However, our numerical experiments demonstrate the ability of the algorithm to cope with modest levels of noise in the data. Another factor in the successful performance of the algorithm is the need for a careful choice of weights in the cost functional and initial guesses for the parameters to be estimated.

In all our numerical experiments we used the reaction–diffusion systems themselves to generate the target patterns via the mechanism of diffusion-driven instability. Ideally, we would like to estimate the model parameters associated with target patterns (\bar{u}, \bar{v}) arising from experimental data. Due to the robustness of the MDOCA algorithm, this should be possible in theory. The MDOCA algorithm should be applicable to a number of well-studied experimental systems. For example, the first experimental evidence of Turing patterns was observed by Lengyel and Epstein [32] in the CIMA chemical reaction, almost 40 years after Turing’s predictions. The CIMA reaction is modeled by a coupled pair of nonlinear reaction–diffusion equations, which in non-dimensional form has four model parameters. In principle, we could apply the MDOCA algorithm to parameterize this system using experimental data; however, this is the subject of future work.

The MDOCA algorithm developed shows great promise as a versatile tool for the mathematical modeling of the Turing mechanism. In particular, it could determine to which parameters model behavior is most sensitive and therefore prioritize which parameters should be the focus of experimental investigation.

Acknowledgments

The authors received partial support from: an NSERC Discovery Grant: RGPIN 340739-2008 (MRG); an Air Force Grant: FA9550-09-1-0058 (CT); and a Royal Society-Wolfson Merit Award (PKM). We also thank Jeff Morgan (University of Houston) for some guidance regarding the proof of the well-posedness of the Schnakenberg system given in the Appendix. The authors also acknowledge the helpful comments of two anonymous referees.

Appendix A

A.1. Well-posedness of the Schnakenberg system

We provide a proof of the well-posedness of the Schnakenberg system using the theoretical setup of Morgan [38].

Theorem A.1. *Let the initial concentrations $(u_0(\mathbf{x}), v_0(\mathbf{x}))$ be bounded and lie in $(0, \infty)^2$ for all $\mathbf{x} \in \Omega$. Then there exists a unique positive classical solution of the Schnakenberg system (1) with kinetics (2) augmented with zero flux boundary conditions for all (\mathbf{x}, t) in $\Omega \times [0, \infty)$.*

Proof. For notational convenience we swap u and v in the Schnakenberg system, which effectively swaps the first and second equations in the reaction kinetics (2), yielding the equivalent system:

$$\begin{cases} \frac{\partial u}{\partial t} = D_u \nabla^2 u + \hat{f}_1(u, v), \\ \frac{\partial v}{\partial t} = D_v \nabla^2 v + \hat{f}_2(u, v), \end{cases}$$

where:

$$\hat{f}_1(u, v) := \gamma(b - v^2 u), \quad \hat{f}_2(u, v) := \gamma(a - v + v^2 u).$$

The local existence of solutions follows from well-known semigroup theory (see for example Pazy [41], or Henry [23]). In particular, from Proposition 1 in Hollis et al. [25] it follows immediately that the Schnakenberg system has an unique non-continuable classical solution (u, v) for $(\mathbf{x}, t) \in \Omega \times [0, T_{max})$. To prove positivity of the solutions observe that the reaction kinetics satisfy:

$$\hat{f}_1(0, v), \hat{f}_2(u, 0) > 0 \quad \text{for all } u, v > 0,$$

and recall that the initial data lie in the positive quadrant of phase space by assumption. Thus by a maximum principle (Smoller [49], Lemma 14.20) the solution $(u(\mathbf{x}, t), v(\mathbf{x}, t))$ lies in $(0, \infty)^2$ for all $\mathbf{x} \in \Omega$ and for all time for which the solution exists. Thus $(0, \infty)^2$ is positively invariant for the system. We apply the theoretical framework of Morgan [38] to prove global existence and uniqueness of classical solutions, which requires ‘intermediate sum’ conditions and polynomial growth conditions on the kinetics to hold.

We first define a so called Lyapunov-type function given by:

$$H(u, v) := h_1(u) + h_2(v), \quad \text{where } h_1(u) = u, \quad h_2(v) = v.$$

Then with $a_{11} = a_{22} = a_{21} = 1$, $K_2 = K_4 = K_6 = \gamma(a + b)$, $K_1 = r = 1$, $K_3 = \gamma/3$, $K_5 = 0$ and $q = 3$ the following conditions are easily verified for all $(u, v) \in (0, \infty)^2$, corresponding to conditions (H4)(i), (H5) and (H6) in Morgan [38], respectively:

$$\begin{aligned} a_{11} h'_1(u) \hat{f}_1(u, v) &\leq K_1 (H(u, v))^r + K_2, \\ a_{21} h'_1(u) \hat{f}_1(u, v) + a_{22} h'_2(v) \hat{f}_2(u, v) &\leq K_1 (H(u, v))^r + K_2, \\ h'_1(u) \hat{f}_1(u, v), \quad h'_2(v) \hat{f}_2(u, v) &\leq K_3 (H(u, v))^q + K_4, \\ \nabla H(u, v) \cdot \begin{pmatrix} \hat{f}_1(u, v) \\ \hat{f}_2(u, v) \end{pmatrix} &\leq K_5 H(u, v) + K_6. \end{aligned}$$

Thus as $r = 1$ Theorems 3.2 and 2.2 in Morgan [38] hold, which implies $T_{max} = \infty$, i.e. we have global existence of positive, classical solutions. \square

A.2. Differentiability of the cost functional J

One can prove that the map $(c_1, c_2) \mapsto (u, v)$ is Gâteaux differentiable and the derivative $\hat{u} = \frac{du}{d(c_1, c_2)}(\hat{c}_1, \hat{c}_2)$, $\hat{v} = \frac{dv}{d(c_1, c_2)}(\hat{c}_1, \hat{c}_2)$ satisfies a linear ‘sensitivity equation’:

$$\begin{aligned} \hat{u}' &= D_u \nabla^2 \hat{u} + \frac{df_1}{d(c_1, c_2)}(u, v), \\ \hat{v}' &= D_v \nabla^2 \hat{v} + \frac{df_2}{d(c_1, c_2)}(u, v). \end{aligned}$$

Furthermore, the optimality of (c_1^*, c_2^*) yields that the derivative of J :

$$\frac{dJ}{d(c_1, c_2)}(\hat{c}_1, \hat{c}_2) = \int_{\Omega} (\gamma_1(u(x, T) - \bar{u}(x)) \hat{u}(x, T) + \gamma_2(v(x, T) - \bar{v}(x)) \hat{v}(x, T)) dx + \delta_1 c_1 \hat{c}_1 + \delta_2 c_2 \hat{c}_2,$$

must be zero on all directions (\hat{c}_1, \hat{c}_2) in the tangent cone of \mathcal{U}_{ad} . When coupling the sensitivities of the state equation and cost functional through the adjoint equation (7), after integration by parts, one obtains the optimality conditions.

References

- [1] A. Ackleh, Parameter estimation in nonlinear evolution equations, *Numer. Funct. Anal. Optim.* 19 (9–10) (1998) 933–947.
- [2] V. Barbu, Analysis and control of nonlinear infinite-dimensional systems, *Mathematics in Science and Engineering*, vol. 190, Academic Press Inc., Boston, MA, 1993.
- [3] R. Barrio, J. Aragón, C. Varea, M. Torres, I. Jiménez, F. Montero de Espinosa, Robust symmetric patterns in the Faraday experiment, *Phys. Rev. E* 56 (4) (1997) 4222–4230.
- [4] A. Borzi, R. Griesse, Experiences with a space-time multigrid method for the optimal control of a chemical turbulence model, *Int. J. Numer. Meth. Fluids* 47 (2005) 879–885.
- [5] A. Borzi, R. Griesse, Distributed optimal control of lambda-omega systems, *J. Numer. Math.* 14 (1) (2006) 17–40.
- [6] A. Borzi, K. Kunisch, A multigrid method for optimal control of time-dependent reaction-diffusion processes, in: *Fast Solution of Discretized Optimization Problems*, International Series of Numerical Mathematics, vol. 138, Birkhäuser, Basel, 2001, pp. 50–57.

- [7] V. Castets, E. Dulos, J. Boissonade, P. De Kepper, Experimental evidence of a sustained Turing-type equilibrium chemical pattern, *Phys. Rev. Lett.* 64 (1990) 2953–2956.
- [8] S. Cerrai, Optimal control problems for stochastic reaction–diffusion systems with non-Lipschitz coefficients, *SIAM J. Control Optim.* 39 (6) (2001) 1779–1816.
- [9] P. Ciarlet, *The finite element method for elliptic problems, Studies in Mathematics and its Applications*, vol. 4, North-Holland Publishing Company, Amsterdam, 1978.
- [10] P. Ciarlet, *Introduction to Numerical Linear Algebra and Optimization*, Cambridge University Press, Cambridge, 1989.
- [11] H. Engl, M. Hanke, A. Neubauer, *Regularization of inverse problems, Mathematics and its Applications*, vol. 375, Kluwer Academic Publishers Group, Dordrecht, 1996.
- [12] R. Filliger, M.-O. Hongler, L. Streit, Connection between an exactly solvable stochastic optimal control problem and a nonlinear reaction–diffusion equation, *J. Optim. Theory Appl.* 137 (3) (2008) 497–505.
- [13] K. Fister, C.M. McCarthy, Optimal control of a chemotaxis system, *Q. Appl. Math.* 61 (2) (2003) 193–211.
- [14] A. Friedman, F. Reitich, Parameter identification in reaction–diffusion models, *Inverse Prob.* 8 (1992) 187–192.
- [15] A. Fursikov, *Optimal control of distributed systems. Theory and applications, Translations of Mathematical Monographs*, vol. 187, American Mathematical Society, Providence, RI, 2000. Translated from the 1999 Russian original by Tamara Rozhkovskaya.
- [16] M. Garvie, C. Trenchea, Optimal control of a nutrient–phytoplankton–zooplankton–fish system, *SIAM J. Control Optim.* 46 (3) (2007) 775–791.
- [17] M. Garvie, C. Trenchea, The identification of space-time distributed parameters in reaction–diffusion systems, in preparation.
- [18] A. Gierer, H. Meinhardt, A theory of biological pattern formation, *Kybernetik* 12 (1972) 30–39.
- [19] R. Griesse, S. Volkwein, A primal–dual active set strategy for optimal boundary control of a nonlinear reaction–diffusion system, *SIAM J. Control Optim.* 44 (2) (2005) 467–494.
- [20] R. Griesse, S. Volkwein, Parametric sensitivity analysis for optimal boundary control of a 3D reaction–diffusion system, in: *Large-Scale Nonlinear Optimization, Nonconvex Optimization and its Applications*, vol. 83, Springer, New York, 2006, pp. 127–149.
- [21] M.D. Gunzburger, *Perspectives in flow control and optimization, Advances in Design and Control*, vol. 5, Society for Industrial and Applied Mathematics (SIAM), Philadelphia, PA, 2003.
- [22] M.D. Gunzburger, S. Manservigi, Analysis and approximation of the velocity tracking problem for Navier–Stokes flows with distributed control, *SIAM J. Numer. Anal.* 37 (5) (2000) 1481–1512.
- [23] D. Henry, *Geometric theory of semilinear parabolic equations, Lecture Notes in Mathematics*, vol. 840, Springer-Verlag, New York, 1981.
- [24] C. Hogue, C. Davatzikos, G. Biros, An image-driven parameter estimation problem for a reaction–diffusion glioma growth model with mass effects, *J. Math. Biol.* 56 (2008) 793–825.
- [25] S. Hollis, R. Martin, M. Pierre, Global existence and boundedness in reaction–diffusion systems, *SIAM J. Math. Anal.* 18 (3) (1987) 744–761.
- [26] V. Isakov, *Inverse problems for partial differential equations, Applied Mathematical Sciences*, second ed., vol. 127, Springer, New York, 2006.
- [27] K. Ito, K. Kunisch, Lagrange multiplier approach to variational problems and applications, *Advances in Design and Control*, vol. 15, Society for Industrial and Applied Mathematics (SIAM), Philadelphia, PA, 2008.
- [28] C.S. Jiang, Y.X. Zhang, A parameter identification and inversion method for a class of reaction–diffusion systems, *Control Theory Appl.* 17 (2) (2000) 193–197.
- [29] C.T. Kelley, *Iterative methods for optimization, Frontiers in Applied Mathematics*, vol. 18, Society for Industrial and Applied Mathematics (SIAM), Philadelphia, PA, 1999.
- [30] S. Kondo, R. Asai, A reaction–diffusion wave on the skin of the marine angelfish *Pomacanthus*, *Nature* 376 (1995) 765–768.
- [31] I. Lasiecka, R. Triggiani, *Control theory for partial differential equations: continuous and approximation theories. I, Encyclopedia of Mathematics and its Applications*, vol. 74, Cambridge University Press, Cambridge, 2000. Abstract parabolic systems.
- [32] I. Lengyel, I. Epstein, Modeling of Turing structures in the chlorite–iodide–malonic acid–starch reaction system, *Science* 251 (1991) 650–652.
- [33] S. Lenhart, J. Workman, *Optimal control applied to biological models, Mathematical and Computational Biology Series*, Chapman & Hall/CRC, London, 2007.
- [34] J.-L. Lions, *Contrôle optimal de systèmes gouvernés par des équations aux dérivées partielles, Avant propos de P. Lelong*, Dunod, Paris, 1968.
- [35] A. Madzvamuse, Time-stepping schemes for moving grid finite elements applied to reaction–diffusion systems on fixed and growing domains, *J. Comput. Phys.* 214 (2006) 239–263.
- [36] H. Meinhardt, *The Algorithmic Beauty of Sea Shells*, fourth ed., Springer-Verlag, Berlin, 2009.
- [37] T. Miura, K. Shiota, G. Morriss-Kay, P. Maini, Mixed mode pattern in Doublefoot mutant mouse limb – Turing reaction–diffusion model on a growing domain during limb development, *J. Theor. Biol.* 240 (2006) 562–573.
- [38] J. Morgan, Global existence for semilinear parabolic systems, *SIAM J. Math. Anal.* 20 (5) (1989) 1128–1144.
- [39] J. Murray, *Mathematical biology II: spatial models and biomedical applications, Interdisciplinary Applied Mathematics*, third ed., vol. 18, Springer-Verlag, New York, 2003.
- [40] Q. Ouyang, H. Swinney, Transition from a uniform state to hexagonal and striped Turing patterns, *Nature* 352 (1991) 610–612.
- [41] A. Pazy, *Semigroups of linear operators and applications to partial differential equations, Applied Mathematical Sciences*, vol. 44, Springer-Verlag, New York, 1983.
- [42] L.S. Pontryagin, V.G. Boltyanskii, R.V. Gamkrelidze, E.F. Mishchenko, *The mathematical theory of optimal processes*, in: L.W. Neustadt (Ed.), *Interscience Publishers John Wiley & Sons, Inc.*, New York, London, 1962. Translated from the Russian by K.N. Trilogoff.
- [43] F. Rothe, *Global solutions of reaction–diffusion systems, Lecture Notes in Mathematics*, vol. 1072, Springer-Verlag, Berlin, 1984.
- [44] J. Ruuth, Implicit–explicit methods for reaction–diffusion problems in pattern formation, *J. Math. Biol.* 34 (1995) 148–176.
- [45] S. Ryu, Boundary control of chemotaxis reaction–diffusion system, *Honam Math. J.* 30 (3) (2008) 469–478.
- [46] J. Schnakenberg, Simple chemical reaction systems with limit cycle behavior, *J. Theor. Biol.* 81 (1979) 389–400.
- [47] L. Segel, J. Jackson, Dissipative structure: an explanation and an ecological example, *J. Theor. Biol.* 37 (1972) 545–559.
- [48] S. Sick, S. Reinker, J. Timmer, T. Schlake, WNT and DKK determine hair follicle spacing through a reaction–diffusion mechanism, *Science* 314 (5804) (2006) 1447–1450.
- [49] J. Smoller, *Shock waves and reaction–diffusion equations, Grundlehren der mathematischen Wissenschaften*, vol. 258, Springer-Verlag, New York, 1983.
- [50] A. Tikhonov, V. Arsenin, *Solutions of Ill-Posed Problems*, V.H. Winston & Sons, John Wiley & Sons, Washington, DC, New York, 1977.
- [51] A. Turing, The chemical basis of morphogenesis, *Philos. Trans. R. Soc. London, Ser. B* 237 (1952) 37–72.
- [52] C. Vogel, *Computational Methods for Inverse Problems, Society for Industrial and Applied Mathematics (SIAM)*, Philadelphia, PA, 2002.